

## Antiferromagnetic interlayer exchange coupling between Fe<sub>3</sub>O<sub>4</sub> layers across a nonmagnetic MgO dielectric layer

Han-Chun Wu,<sup>1,a)</sup> S. K. Arora,<sup>1</sup> O. N. Mryasov,<sup>2,b)</sup> and I. V. Shvets<sup>1</sup>

<sup>1</sup>CRANN and School of Physics, Trinity College Dublin, Dublin 2, Ireland

<sup>2</sup>Seagate Technology, Pittsburgh, 1251 Waterfront PL., Pennsylvania 15222, USA

(Received 24 January 2008; accepted 12 April 2008; published online 7 May 2008)

We have investigated the interlayer exchange coupling between the epitaxial spinel Fe<sub>3</sub>O<sub>4</sub> layers across an insulating nonmagnetic MgO spacer. The epitaxial structure used for these investigations was Fe<sub>3</sub>O<sub>4</sub> (10 nm)/MgO (0.8–3 nm)/Fe<sub>3</sub>O<sub>4</sub> (10 nm)/NiO (15 nm) multilayers grown on MgO (100) substrates. We find that the two Fe<sub>3</sub>O<sub>4</sub> layers are antiferromagnetic coupled through the MgO spacer when the MgO thickness is less than 1.5 nm. Furthermore, *ab initio* calculation of IEC for Fe/MgO/Fe indicates the importance of electrode states, in particular, partial oxidation of the ferromagnetic electrodes. © 2008 American Institute of Physics. [DOI: 10.1063/1.2919081]

Over the last few decades, magnetite has been attracting a tremendous amount of attention owing to its high Curie temperature of 858 K and its half metallic nature.<sup>1,2</sup> These properties make it an important candidate for magnetic tunnel junctions (MTJs) and spin valves. However, initial efforts in exploiting its half metallic nature in MTJ have been far from promising.<sup>3–5</sup> The tunnel magnetoresistance (TMR) below the expectations attained in these investigations was attributed to the formation of a dead layer at the interface between Fe<sub>3</sub>O<sub>4</sub> and MgO layers. However, other sources affecting the TMR in such structures, such as interface roughness, interlayer exchange coupling (IEC) between the ferromagnetic (FM) electrodes across an insulating spacer, etc., cannot be ruled out.<sup>5</sup>

The IEC across an insulating nonmagnetic spacer is expected to be nonoscillatory and exponentially decrease with increasing the spacer thickness. In earlier investigations, IEC across a nonmagnetic dielectric invariably observed had FM nature.<sup>6,7</sup> Possibly, the fact that antiferromagnetic (AF) IEC was not observed was related to deficiencies in the control of interface roughness, and thus, orange peel effect, pinholes, and the use of amorphous Al<sub>2</sub>O<sub>3</sub> barrier. Recently, Faure-Vincent *et al.*<sup>8</sup> found a strong AF IEC in a fully epitaxial Fe/MgO/Fe trilayer structure. The IEC for Fe<sub>3</sub>O<sub>4</sub>/MgO/Fe<sub>3</sub>O<sub>4</sub> trilayers was investigated by van der Heijden *et al.*<sup>9</sup> and they found that the coupling is FM. Below 1.3 nm of MgO thickness, the coupling is due to the presence of pinholes and for greater thickness is due to orange peel coupling effect. In their studies, polished substrates having scratches were used, which gave rise to defects as evidenced both in scanning tunneling microscopy and indirectly in the behaviour of MTJs.<sup>10</sup> This prompted us to investigate the IEC of the magnetite-based epitaxial trilayer structures. We should stress that apart from Fe<sub>3</sub>O<sub>4</sub>, the MgO tunnel barrier is crucially important to the field of TMR and application of MTJ.<sup>11</sup> Therefore, further understanding of its IEC behavior is of high importance. In this letter, we report on the measurements of the magnetic properties of Fe<sub>3</sub>O<sub>4</sub>/MgO/Fe<sub>3</sub>O<sub>4</sub>/NiO multilayers epitaxially grown on MgO (100) substrates. We found that two Fe<sub>3</sub>O<sub>4</sub> layers are

AF coupled through MgO spacer for up to 1.5 nm spacer thickness.

Our study is performed on a fully epitaxial Fe<sub>3</sub>O<sub>4</sub>/MgO/Fe<sub>3</sub>O<sub>4</sub>/NiO/MgO (100) stack. The thickness of both the Fe<sub>3</sub>O<sub>4</sub> layers was 10 nm and that of the MgO spacer was varied between 0.8 and 3 nm. The said stacks were grown on MgO (100) single crystal substrates by molecular beam epitaxy (MBE). Details of the growth conditions used for Fe<sub>3</sub>O<sub>4</sub> layers are given elsewhere.<sup>12</sup> The NiO (15 nm) epilayer was deposited at a substrate temperature of 600 °C with an oxygen partial pressure 5 × 10<sup>-6</sup> Torr. After the NiO growth, the sample was cooled to 250 °C and a 10 nm film of Fe<sub>3</sub>O<sub>4</sub> was grown to serve as the bottom FM layer. Then, a single crystalline MgO (100) layer was formed at 250 °C with a rather low deposition rate 0.05 Å/s and annealed at 250 °C for 20 min in a vacuum of 5 × 10<sup>-9</sup> Torr. Subsequently, the second (top) Fe<sub>3</sub>O<sub>4</sub> layer was deposited.

Figure 1 shows the representative reflection high energy

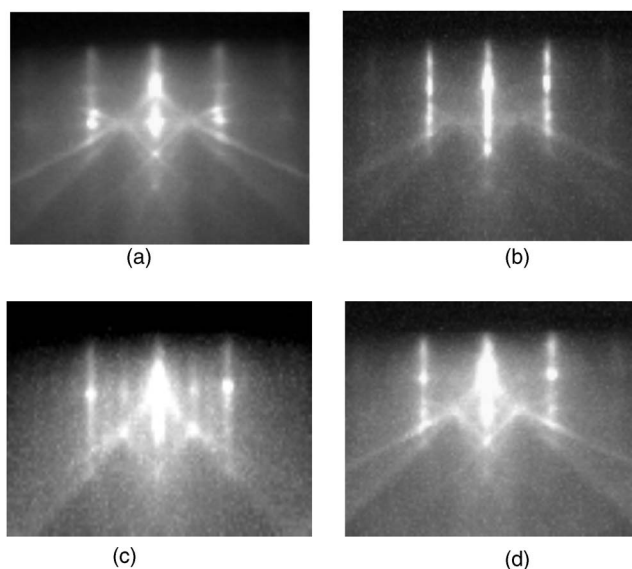


FIG. 1. RHEED images of (a) UHV annealed substrate, (b) after 15 nm NiO growth on MgO, (c) after 10 nm Fe<sub>3</sub>O<sub>4</sub> growth on NiO/MgO, and (d) after 8 Å MgO growth on Fe<sub>3</sub>O<sub>4</sub>/NiO/MgO. The images were recorded in (100) azimuth.

<sup>a)</sup>Electronic mail: wuhc@tcd.ie.

<sup>b)</sup>Electronic mail: oleg.mryasov@seagate.com.

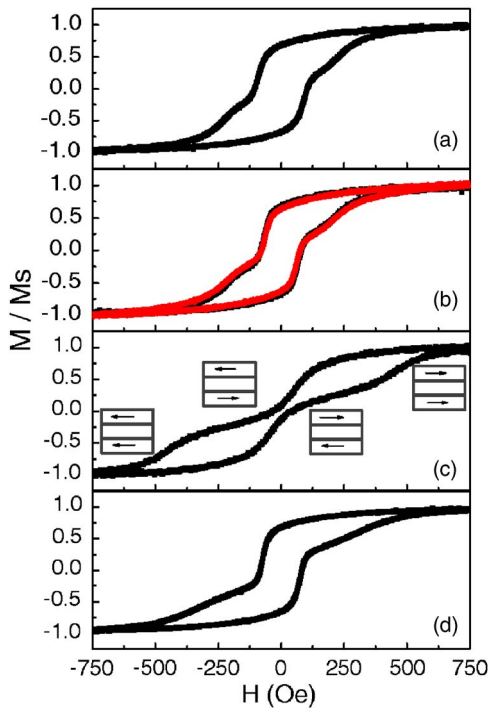


FIG. 2. (Color online) Magnetic HLs of  $\text{Fe}_3\text{O}_4/\text{MgO}/\text{Fe}_3\text{O}_4/\text{NiO}$  multilayers measured at 300 K for different MgO thickness. The thickness of MgO spacer are (a) 3 nm, (b) 2.5 nm (black line) and 2 nm (red line), (c) 0.8 nm, and (d) 1.5 nm, respectively.

electron diffraction (RHEED) patterns recorded in (100) azimuth during growth. The patterns for substrate [Fig. 1(a)] and MgO spacer [Fig. 1(d)] show vertical lattice rods and sharp Kikuchi lines representative of well ordered and smooth surface. Figure 1(b) is the RHEED image after the growth of 15 nm NiO on MgO surface. One can see that the NiO epitaxially grew on MgO substrate. Figure 1(c) shows the RHEED image after the growth of 10 nm  $\text{Fe}_3\text{O}_4$  film on NiO/MgO. Half order streaks corresponding to the magnetite unit cell appear between the locations of MgO or NiO lattice rods, which indicates pseudomorphic growth of  $\text{Fe}_3\text{O}_4$ . We should mention that, for both the top and bottom 10 nm  $\text{Fe}_3\text{O}_4$  FM layer, Verwey transition was at 115 K both from magnetization versus temperature and resistivity versus temperature measurements.

The magnetic properties of  $\text{Fe}_3\text{O}_4/\text{MgO}/\text{Fe}_3\text{O}_4/\text{NiO}$  multilayers at 300 K were examined by alternating gradient field magnetometer. The magnetic field was applied in the films plane along the  $\langle 001 \rangle$  direction. Figure 2(a) shows the magnetic hysteresis loop (HL) measured for the MgO layer thickness of 3 nm. At this thickness, the exchange interaction between the  $\text{Fe}_3\text{O}_4$  layers is broken due to the relatively thick MgO spacer and this makes interpretation of the data easier. There are two coercive fields ( $H_{c1}=61$  Oe and  $H_{c2}=235$  Oe) that correspond to the coercivity of  $\text{Fe}_3\text{O}_4$  layers grown on MgO and NiO, respectively. The presence of an NiO underlayer causes the coercivity of the bottom  $\text{Fe}_3\text{O}_4$  layer to marginally increase due to the weak exchange bias effect. This weak exchange bias is due to the fact that the samples were not field cooled in connection to the small anisotropy of NiO.<sup>13</sup> This view is confirmed by the HL for the MgO layer thicknesses of 2.5 and 2 nm [Fig. 2(b)]. The situation becomes very interesting once the thickness of MgO spacer falls below 2 nm. Figure 2(c) shows the HL for the MgO

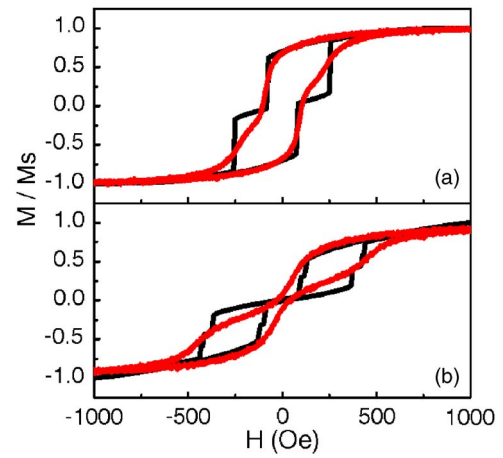


FIG. 3. (Color online) Black lines are the simulated HLs calculated in the absence of any IEC (a) between two  $\text{Fe}_3\text{O}_4$  layers and for the case of the (b) two  $\text{Fe}_3\text{O}_4$  layers AF coupled through a 0.8 nm MgO layer. The red lines are the experimental HLs for the MgO spacer of (a) 3 nm and (b) 0.8 nm.

thickness of 0.8 nm. Remarkably, the overall value  $M_r$  of the magnetic moment of the trilayer at zero field is reduced to 9%. The unusual HL can be explained by AF IEC between the two  $\text{Fe}_3\text{O}_4$  layers. The arrangement of the magnetic moments of the two layers is schematically shown in Fig. 2(c). At the thickness of 1.5 nm of MgO, the AF IEC is still visible, as shown in Fig. 2(d).

We have simulated the HL of  $\text{Fe}_3\text{O}_4/\text{MgO}/\text{Fe}_3\text{O}_4/\text{NiO}$  by means of the micromagnetic calculation (OOMMF code).<sup>14</sup> The system we considered consists of two magnetic thin films with the same thickness but different coercive fields ( $H_{c1}$  and  $H_{c2}$ ). The model of magnetic interactions include five types of energies, which are the exchange energy  $E_{xc}$ , IEC energy  $E_{IEC}$ , anisotropy energy  $E_{anis}$ , magnetostatic energy  $E_{demag}$ , and Zeeman energy  $E_{Zeeman}$ . The magnetic free energy per unit volume of cell  $i$  is given by the following:

$$E = \frac{A}{M_S^2} (|\nabla M_x|^2 + |\nabla M_y|^2 + |\nabla M_z|^2) + \sum_{j'} \frac{J_1 [1 - (m_i \cdot m_{j'})] + J_2 [1 - (m_i \cdot m_{j'})^2]}{\Delta_{ij'}} + E_{anis} + E_{demag} + E_{Zeeman}, \quad (1)$$

where first two terms are explicit expressions for intralayer  $E_{xc}$  and interlayer  $E_{IEC}$  exchange contributions. Here,  $J_1$  and  $J_2$  are the IEC interaction parameters,  $m_i$  and  $m_{j'}$  are the normalized spins at cells  $i$  and  $j'$ , and  $\Delta_{ij'}$  is the discretization step size between cell  $i$  and cell  $j'$ . These parameters for magnetite are magnetization saturation  $M_S=4.85 \times 10^5$  A/m, exchange stiffness  $A=1.32 \times 10^{-11}$  J/m, cubic anisotropy  $K_1=-1.36 \times 10^4$  J/m<sup>3</sup>, and IEC interaction parameter  $J_1$ , which is treated in our modeling as an adjustable parameter. The dimensions of the two magnetic thin films in our simulations are taken as  $500 \times 500 \times 10$  nm<sup>3</sup>. These simulations are summarized in Fig. 3 showing that the IEC between the two  $\text{Fe}_3\text{O}_4$  layers is  $J_1=-4.6 \times 10^{-5}$  J/m<sup>2</sup> for the MgO spacer thickness of 0.8 nm. The observed stark AF IEC in our case is in strong contrast to that reported by van der Heijden *et al.*<sup>9</sup>

The origin of IEC via tunneling barrier is often explained either in terms of the spin torque<sup>15</sup> or in terms of

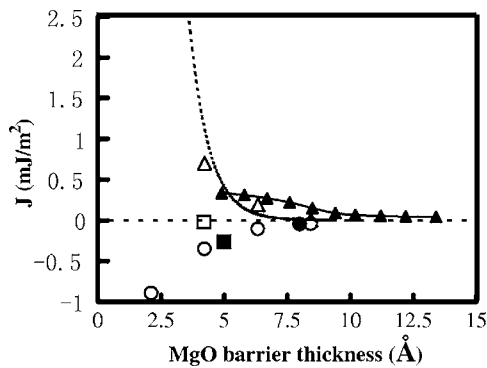


FIG. 4. Calculated IEC  $J$  for ideal (open triangles) Fe/MgO/Fe junction and for the cases of oxidized Fe (open dots) and MgO barrier with vacancy (open square). Experimental points are (i) present work for Fe<sub>3</sub>O<sub>4</sub>/MgO(0.8 nm)/Fe<sub>3</sub>O<sub>4</sub> (filled dot), (ii) Ref. 9 for a series of MgO thicknesses (filled triangles), and (iii) Ref. 8 for MBE grown Fe/MgO(0.5 nm)/Fe (filled square).

electron waves interference in the barrier.<sup>16</sup> Recently, it has been shown that, depending on the position of an impurity level in the barrier, IEC may change sign from what it is in an ideal tunneling junction.<sup>17</sup> This result suggests the possibility of an AF IEC through a wide-band-gap barrier such as MgO, is due to defects in the barrier. The drawback of above theoretical considerations is in the use of the free electron model to describe spin polarized tunneling and virtual insensitivity of these models to FM electrodes. More recently, an *ab initio* electronic structure method has been used to investigate barrier vacancy mediated IEC in Fe/MgO/Fe junctions.<sup>18</sup> The authors advocate vacancies in the barrier as the origin of AF IEC observed in Fe/MgO/Fe junctions. However, a large concentration of vacancies in these calculations is not supported by experimental results. It seems more reasonable to expect a higher concentration of interstitial oxygen or partial oxidation at the interface between the FM electrodes and MgO than vacancies. Note that one may consider our system Fe<sub>3</sub>O<sub>4</sub>/MgO/Fe<sub>3</sub>O<sub>4</sub> as an extreme case of oxidized FM electrodes in Fe/MgO/Fe MTJs. Having that in mind and to elaborate further on the role of defects, we have performed *ab initio* calculations of IEC for the Fe/MgO/Fe junction with a variable thickness of MgO barrier. We employed *ab initio* tight binding model that is suitable to describe strongly bonded MgO tunneling barrier. This model is based on the so-called linearized muffin tin orbital method in the atomic sphere approximation (LMTO-ASA).<sup>19</sup> To model effect of electrode oxidation, we introduced interstitial oxygen at Fe/MgO interface, while for effect of MgO oxygen vacancy, we used the 2×2 supercell. We compare the effect of two defects on IEC, vacancy in the barrier and interface Fe oxidation. To determine IEC, we use constrained density functional theory and generalization of LMTO-ASA method to describe noncollinear magnetic configurations.<sup>20</sup> These calculations are summarized in Fig. 4 showing exponentially decaying positive IEC for ideal Fe/MgO/Fe junctions and a change of IEC sign for partially oxidized FM/MgO interfaces. These results indicate that the distribution of

oxygen within FM electrode in the tunneling junction may have a more pronounced effect on IEC than vacancies in the tunneling barrier.

In summary, we have investigated the magnetic properties of epitaxially grown Fe<sub>3</sub>O<sub>4</sub>/MgO/Fe<sub>3</sub>O<sub>4</sub>/NiO multilayers, for varying thicknesses of the MgO spacer. AF IEC between Fe<sub>3</sub>O<sub>4</sub> layers through MgO spacer has been unambiguously evidenced. Surprisingly, it persists up to the large thickness of MgO spacer of 1.5 nm. Our *ab initio* calculation of IEC for Fe/MgO/Fe further indicates the importance of the electrode state, in particular, the partial oxidation of the FM electrodes.

This work was supported by the SFI under Contract No. 06/IN.1/191. O.N.M. is grateful to the SFI C.T. Walton fellowship support during his stay at TCD. We are grateful to Dr. Heinonen for useful discussion.

- <sup>1</sup>F. Walz, *J. Phys.: Condens. Matter* **14**, R285 (2002).
- <sup>2</sup>M. Ziese, *Rep. Prog. Phys.* **65**, 143 (2002); J. H. V. J. Brabers, F. Walz, and H. Kronmüller, *J. Phys.: Condens. Matter* **12**, 5437 (2002).
- <sup>3</sup>K. Ghosh, S. B. Ogale, S. P. Pai, M. Robson, E. Li, I. Jin, Z. W. Dong, R. L. Greene, R. Ramesh, T. Venkatesan, and M. Johnson, *Appl. Phys. Lett.* **73**, 689 (1998).
- <sup>4</sup>P. Sensor, A. Fert, J. L. Maurice, F. Montaigne, F. Petroff, and A. Vaurs, *Appl. Phys. Lett.* **74**, 4017 (1999).
- <sup>5</sup>X. W. Li, A. Gupta, G. Xiao, W. Qian, and V. P. Dravid, *Appl. Phys. Lett.* **73**, 3282 (1998).
- <sup>6</sup>E. Y. Tsymlal, O. N. Mryasov, and P. R. LeClair, *J. Phys.: Condens. Matter* **15**, R109 (2003).
- <sup>7</sup>J. D. R. Buchanan, T. P. A. Hase, B. K. Tanner, N. D. Hughes, and R. J. Hicken, *Appl. Phys. Lett.* **81**, 751 (2002).
- <sup>8</sup>J. Faure-Vincent, C. Tiusan, C. Bellouard, E. Popova, M. Hehn, F. Montaigne, and A. Schuhl, *Phys. Rev. Lett.* **89**, 107206 (2002).
- <sup>9</sup>P. A. A. van der Heijden, P. J. H. Bloemen, J. M. Metselaar, R. M. Wolf, J. M. Gaines, J. T. W. M. van Eemeren, P. J. van der Zaag, and W. J. M. de Jonge, *Phys. Rev. B* **55**, 11569 (1997).
- <sup>10</sup>P. J. van der Zaag, P. J. H. Bloemen, J. M. Gaines, R. M. Wolf, P. A. A. van der Heijden, R. J. M. van de Veerdonk, and W. J. M. de Jonge, *J. Magn. Magn. Mater.* **211**, 301 (2000), and references therein.
- <sup>11</sup>S. S. P. Parkin, C. Kaiser, A. Panchula, P. M. Rice, B. Hughes, M. Samant, and S. H. Yang, *Nat. Mater.* **3**, 862 (2004); S. Yuasa, T. Nagahama, A. Fukushima, Y. Suzuki and K. Ando, *ibid.* **3**, 868 (2004).
- <sup>12</sup>S. K. Arora, R. G. S. Sofin and I. V. Shvets, *Phys. Rev. B* **72**, 134404 (2005).
- <sup>13</sup>P. J. van der Zaag, A. R. Ball, L. F. Feiner, R. M. Wolf, and P. A. A. van der Heijden, *J. Appl. Phys.* **79**, 5103 (1996).
- <sup>14</sup>M. J. Donahue and D. G. Porter, "OOMMF User's Guide, version 1.2a," National Institute of Standards and Technology, Technical Report No. NISTIR 6376, Gaithersburg, MD, 1999 (<http://math.nist.gov/oommf>).
- <sup>15</sup>J. C. Slonczewski, *Phys. Rev. B* **39**, 6995 (1989); R. Erickson, K. Hathaway, and J. Cullen, *ibid.* **47**, 2626 (1993).
- <sup>16</sup>P. Bruno, *J. Magn. Magn. Mater.* **121**, 248 (1993); P. Bruno, *Phys. Rev. B* **52**, 411 (1995).
- <sup>17</sup>M. Y. Zhuravlev, E. Y. Tsymlal, and A. V. Vedyayev, *Phys. Rev. Lett.* **94**, 026806 (2005).
- <sup>18</sup>M. Zhuravlev, J. Velev, A. Vedyayev, and E. Tsymlal, *J. Magn. Magn. Mater.* **300**, 277 (2006); T. Katayama, S. Yuasa, J. Velev, M. Y. Zhuravlev, S. S. Jaswal, and E. Y. Tsymlal, *Appl. Phys. Lett.* **89**, 112503 (2006).
- <sup>19</sup>O. K. Andersen and O. Jepsen, *Phys. Rev. Lett.* **53**, 2571 (1984).
- <sup>20</sup>O. N. Mryasov, V. A. Gubanov, and A. I. Liechtenstein, *Phys. Rev. B* **45**, 12330 (1992).